

From Modular to Centralized Organization of Synchronization in Functional Areas of the Cat Cerebral Cortex

Jesús Gómez-Gardeñes^{1,2*}, Gorka Zamora-López³, Yamir Moreno^{1,4}, Alex Arenas^{1,5}

1 Instituto de Biocomputación y Física de Sistemas Complejos (BIFI), Universidad de Zaragoza, Zaragoza, Spain, **2** Departamento de Matemática Aplicada, Universidad Rey Juan Carlos (ES CET), Móstoles (Madrid), Spain, **3** Interdisciplinary Center for Dynamics of Complex Systems, University of Potsdam, Potsdam, Germany, **4** Departamento de Física Teórica, Universidad de Zaragoza, Zaragoza, Spain, **5** Departament d'Enginyeria Informàtica y Matemàtiques, Universitat Rovira i Virgili, Tarragona, Spain

Abstract

Recent studies have pointed out the importance of transient synchronization between widely distributed neural assemblies to understand conscious perception. These neural assemblies form intricate networks of neurons and synapses whose detailed map for mammals is still unknown and far from our experimental capabilities. Only in a few cases, for example the *C. elegans*, we know the complete mapping of the neuronal tissue or its mesoscopic level of description provided by cortical areas. Here we study the process of transient and global synchronization using a simple model of phase-coupled oscillators assigned to cortical areas in the cerebral cat cortex. Our results highlight the impact of the topological connectivity in the developing of synchronization, revealing a transition in the synchronization organization that goes from a modular decentralized coherence to a centralized synchronized regime controlled by a few cortical areas forming a Rich-Club connectivity pattern.

Citation: Gómez-Gardeñes J, Zamora-López G, Moreno Y, Arenas A (2010) From Modular to Centralized Organization of Synchronization in Functional Areas of the Cat Cerebral Cortex. PLoS ONE 5(8): e12313. doi:10.1371/journal.pone.0012313

Editor: Olaf Sporns, Indiana University, United States of America

Received: July 23, 2010; **Accepted:** July 29, 2010; **Published:** August 26, 2010

Copyright: © 2010 Gómez-Gardeñes et al. This is an open-access article distributed under the terms of the Creative Commons Attribution License, which permits unrestricted use, distribution, and reproduction in any medium, provided the original author and source are credited.

Funding: J.G.-G. is supported by the Spanish Ministerio de Ciencia e Innovación (MICINN) through projects FIS2008-01240 and MTM2009-13848. G.Z.-L. is supported by the Deutsche Forschungsgemeinschaft, research group FOR 868 (KU 837/23-1) and the BioSim network of excellence (LSHB-CT-2004-005137). Y.M. is supported by Spanish MICINN through projects FIS2008-01240 and FIS2009-13364-C02-01. A.A. acknowledges partial support by the Director, Office of Science, Computational and Technology Research, U.S. Department of Energy under Contract DE-AC02-05CH11231 and the Spanish MICINN through project FIS2009-13730-C02-02. The funders had no role in study design, data collection and analysis, decision to publish, or preparation of the manuscript.

Competing Interests: The authors have declared that no competing interests exist.

* E-mail: gardenes@gmail.com

Introduction

Processing of information within the nervous system follows different strategies and time-scales. Particular attributes of the sensory stimuli are transduced into electrical signals of different characteristics, e.g. regular or irregular spiking, the rate of firing, etc. Further aspects of the information are “encoded” by specialization of neurons, e.g. the color and orientation of a visual stimulus will activate only a set of neurons and leave others silent. For higher order processes such as feature binding and association, the synchronization between neural assemblies plays a crucial role [1–5]. For example, subliminal stimulation which is not consciously perceived, triggers a similar cascade of activation in the sensory system but fails to elicit a transient synchronization between distant cortical regions [6].

The neurons comprising the nervous system form a complex network of communications. To what extent this intricate architecture supports the richness and complexity of the ongoing dynamical activity in the brain is a fundamental question [7]. A detailed map of the neurons and their synapses in mammals is still unknown and far from our experimental capabilities. Only in a few cases, for example the nematode *C. elegans*, we know the complete mapping of the neuronal tissue. In the cases of macaque monkeys and cats a mesoscopic level of description is known, composed of cortical areas and the axonal projections between

them. These areas are arranged into modules which closely follow functional subdivisions by modality [8–13]. Two cortical areas are more likely connected if both are involved in the processing of the same modal information (visual, auditory, etc.) Beyond this modular organization, some cortical areas are extensively connected (referred as *hubs*) with projections to areas in all modalities [14,15]. For the corticocortical network of cats, these hubs are found to be densely interconnected forming a *hidden* module [16], at the top of the cortical hierarchy which might be responsible for the integration of multisensory information. A core of cortical areas has also been detected in estimates of human corticocortical connectivity by Diffusion Spectrum Imaging [17]. Following the above discussion that synchronization plays a major role in the processing of high level information, it would be important to analyze the synchronization behavior of these networks in relation to their modular and hierarchical organization. To this end, we simulate the corticocortical network of the cat by non-identical phase oscillators and we follow the evolution of their synchronization from local to global.

The study of synchronization phenomena is a useful tool to analyze the substrate of complex networks. The dynamical patterns under different parameters unveil features of the underlying microscopic and mesoscopic organization [18]. In particular, recent studies highlight the impact that the topological properties such as the degree heterogeneity, the small-world effect

and the modular structure have on the path followed from local to global synchronization [18–21].

In this work we study the routes to synchronization in the corticocortical network of cats brain (see Figure 1) by modelling each cortical area as a phase oscillator with an independent internal frequency. This assumption considers that the ensemble of neurons contained within a cortical area behaves coherently having a well defined phase average whose dynamics is described by the internal frequency [22]. The coupling between areas is modelled using the Kuramoto nonlinear coupling and its relative strength can be conveniently tuned to allow for the observation of synchronization at different scales of organization. This seemingly crude approximation allows to obtain similar synchronization patterns as those observed with more refined models based on neuronal ensembles placed at each cortical area [23–25]. For instance, using the Kuramoto model one obtains that highly connected areas promote synchronization of neural activity just as revealed by the more stylized model used for the dentate gyrus [26].

Our results point out that complex structures of highly connected areas play a key role in the synchronization transition. In contrast to the usual partition of the brain cortex into four sets of modally-related areas, we find that this modular organization plays a secondary role in the emergence of synchronization patterns. On the contrary, we unveil that a new module made up of highly connected areas (not necessarily modally-related) drives the dynamical organization of the system. This new set is seen as the Rich-Club of the corticocortical network. Surprisingly, the new partition of the network including the Rich-Club as a module preserves the modular behavior of the system’s dynamics at low intercortical coupling strengths. This modular behavior transforms into a centralized one (driven by the Rich-Club) at the onset of global synchronization highlighting the plasticity of the network to perform specialized (modular) or integration (global) tasks depending on the coupling scale.

Results

As introduced above, we describe the dynamical behavior of the cortical network using the Kuramoto model [27], where the time

evolution of the phase of each cortical area, $\theta_i(t)$, is given by

$$\dot{\theta}_i = \omega_i + \lambda \sum_{j=1}^N W_{ij} \sin(\theta_j - \theta_i), \tag{1}$$

where ω_i is the internal frequency associated to area i and W_{ij} is the weighted inter-cortical coupling matrix that takes a value 0 if area j does not interact with the dynamics of area i while $W_{ij} > 0$ otherwise. In this latter case W_{ij} can take values 1, 2 or 3 depending on the axon density going from area j to area i . Let us remark that the inter-cortical coupling matrix is not symmetric so that in general $W_{ij} \neq W_{ji}$. Besides, the inter-cortical dynamical coupling is modeled as the sine of the phase differences between two connected areas such that when $\theta_j > \theta_i$ the average phase of area i accelerates while that of area j slows down to approach each other. Finally, the parameter λ accounts for the strength of the inter-cortical coupling.

In a system composed of all-to-all coupled oscillators, the Kuramoto model shows a transition from incoherent dynamics to a synchronized regime as λ increases [28,29]. However, when the system has a nontrivial underlying structure this transition does not take place in an homogeneous manner. In complex topologies, and for moderate coupling values, certain parts of the system become synchronized rather fast whereas other regions still behave incoherently. Therefore, one can monitor the synchronization patterns that appear as the coupling λ is increased and describe the path to synchronization accurately [18] by reconstructing the synchronized subgraph composed of those nodes and links that share the largest degree of synchronization (see Materials and Methods). The study of these synchronization clusters as the coupling λ is increased allow to unveil the important set of nodes that drives these dynamical processes in the system.

We will analyze different scales of organization: *i*) the macroscopic scale referring to global synchronization of the network; *ii*) the microscopic scale of organization corresponding to the individual state of the oscillators; and finally *iii*) the intermediate mesoscopic scale of dynamical organization between the macroscopic and microscopic scales. Usually, it consists of groups of nodes classified

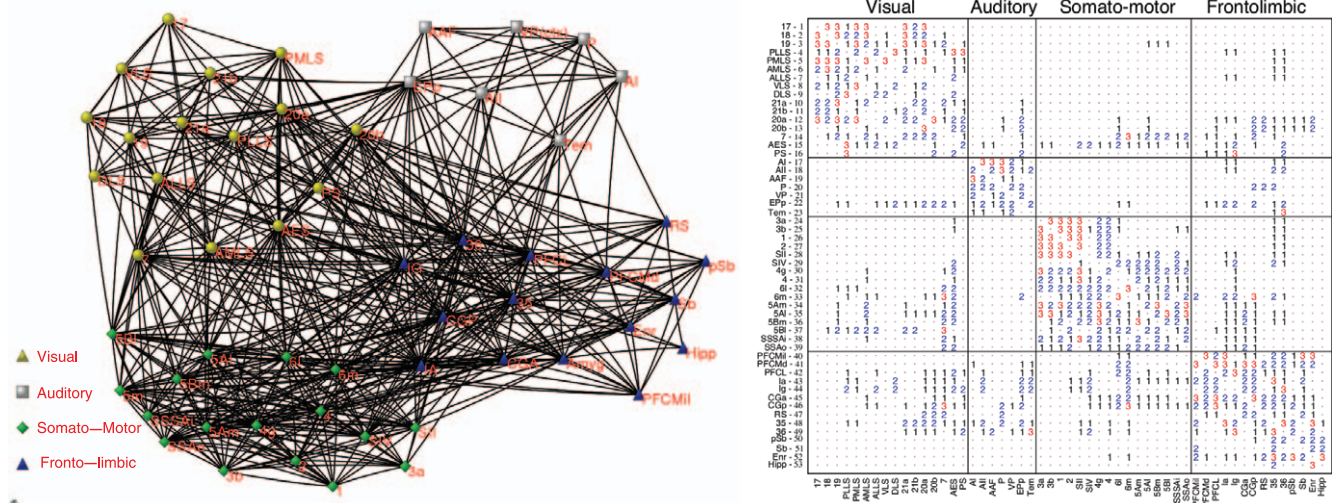


Figure 1. The brain cortical network of the cat. On the left we show the topology of the nodes (areas) and links (axon interconnections) between them. On the right the weighted adjacency matrix is shown. The weight of the links denote the axon density between two connected areas. Besides the matrix shows the partition of the network into four main modules of modally-related areas: Visual, Auditory, Somatosensory-Motor and Fronto-Limbic.

doi:10.1371/journal.pone.0012313.g001

according to a certain additional information, for example that provided by the anatomico-functional modules. Every scale of organization requires a particular set of statistical descriptors. This is especially important in the mesoscopic scale where changing the groups, the characterization of the system is also changed.

Macroscopic analysis

We start by describing how global synchronization is attained as the inter-cortical coupling λ is increased. Global synchronization is characterized by the usual Kuramoto order parameter, r , and the fraction of links that are synchronized r_{link} [20,21] (see Materials and Methods). Both parameters take values in the region $[0, 1]$, being close to 0 when no dynamical coherence is observed and close to 1 when the system approaches to full synchronization.

In Fig. 2 we show the evolution of r and r_{link} as a function of λ . The plot reveals a well defined transition from incoherent to globally synchronized, the onset of synchronization occurring for coupling strength $0.011 \leq \lambda \leq 0.021$. When $\lambda \simeq 0.2$, the system reaches the fully synchronized state. In the following, we will explore this transition in more detail and at lower scales of dynamical organization.

Mesoscopic analysis as described by the four anatomical modules

The measures r and r_{link} describe completely the dynamical state of the system if one assumes that all the cortical areas behave identically. However, it is possible to extract more information about the local dynamical properties of the system. In particular, for a given value of λ we can monitor the degree of synchronization between two given areas i and j , $r_{ij} \in [0, 1]$ (see Materials and Methods).

The studies of the transition to synchronization in modular architectures [19,21] show that synchrony patterns appear first at internal modules, *i.e.* synchrony shows up among the nodes that belong to the same module due to a larger local density within the module and similar pattern of inputs of the nodes. As the coupling λ is increased, synchrony starts to affect the links connecting nodes

of different clusters and finally spreads to the entire system. Now, we analyze whether the four anatomico-functional modules of the corticocortical network of the cat act also as dynamical clusters in the synchronization transition. To this end, we have analyzed the evolution of the average synchronization within and between the four anatomical modules taking into account solely the information about the dynamical coherence r_{ij} between the network's areas. We define the average synchronization between module α and module β as:

$$r_{\alpha\beta} = \frac{1}{L_{\alpha\beta}} \sum_{i \in \alpha, j \in \beta} r_{ij}, \quad (2)$$

where $L_{\alpha\beta}$ is the number of possible pairs of areas from modules α and β , *i.e.*, $L_{\alpha\beta} = N_{\alpha}N_{\beta}/2$ where N_{α} and N_{β} are the number of areas of modules α and β respectively. If $\alpha = \beta$ equation (2) denotes the intramodule average synchronization.

The histograms in the left columns of Figure 3 and Figure 4 show the values of the set $\{r_{\alpha\beta}\}$ for several values of λ corresponding to the region before (Fig. 3) and at (Fig. 4) the onset of synchronization. From the histograms it is clear that the degree of synchronization grows with λ as it occurs for the global parameters r and r_{link} in the macroscopic description. Besides, the histograms inform us about the importance of the anatomical partition in the dynamical organization of the cat cortex. From Figure 3 it becomes clear that the average dynamical correlation within areas of the same anatomical module is higher than that between areas belonging to different modules. Moreover, before the onset of synchronization, for $\lambda = 0.007$ to $\lambda = 0.11$ all the modules satisfy $r_{\alpha\alpha} \geq r_{\alpha\beta}$ for $\alpha \neq \beta$. At the onset of synchronization (left column of Figure 4) we observe that the initial intra-module synchronization is progressively compensated by the increase of inter-module dynamical coherence. In particular, the influence of the Somatosensory-Motor on the remaining modules is remarkably relevant during the onset of synchronization and, for $\lambda > 0.021$, this module shows the largest degree of synchronization with the rest of the system.

Microscopic analysis: Unveiling the dynamical organization

The mesoscopic analysis based on the partition of the cortex into four modules has revealed a fingerprint of a hierarchical organization of the synchronization based on the dominating role of the Somatosensory-Motor module. Here we will analyze the microscopic correlation between all the areas of the cortical network to unveil whether there is a group of nodes that lead the onset of synchronization in the system. To this purpose we study the subgraphs formed by those pairs of areas sharing an average synchronization value r_{ij} larger than a threshold T . Certainly when $T = 1$ the subgraph is the null (empty) graph and for $T = 0$ the subgraph is the whole cortex.

In Figure 5 we show a ranking of the cortical areas at coupling strengths $\lambda = 0.015, 0.017, 0.019$ and 0.021 corresponding to the onset of synchronization. The rankings are made by labeling the area i with the largest value of the threshold at which the area is incorporated into the synchronized subgraph as T is tuned from 1 to 0. Additionally, the modular origin of the areas has been color coded to distinguish the role of each module. From the rankings we find that there are three areas 36, 35 and Ig, from the Fronto-Limbic system, that share the largest degree of synchrony. In all the cases, several jumps in the threshold are observed that distinguishes those groups of cortical areas that are more synchronized than

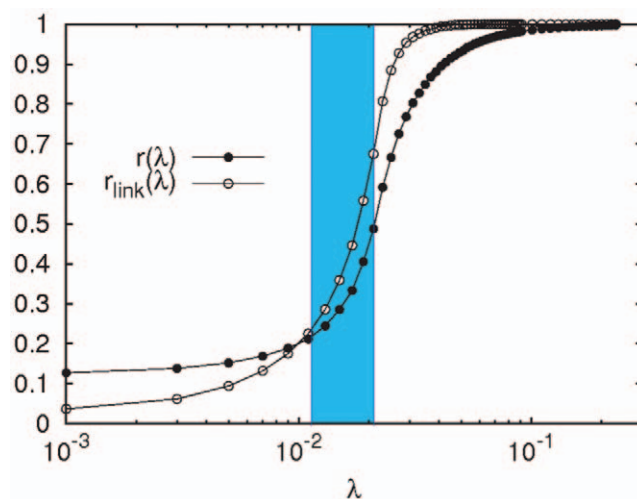


Figure 2. Synchronization diagrams. The figure shows the evolution of the Kuramoto order parameter r and the fraction of synchronized links r_{link} as the coupling strength is increased. The transition from asynchronous dynamics to global dynamical coherence as λ grows is clear from the two curves. The region in blue corresponds to the onset of synchronization.

doi:10.1371/journal.pone.0012313.g002

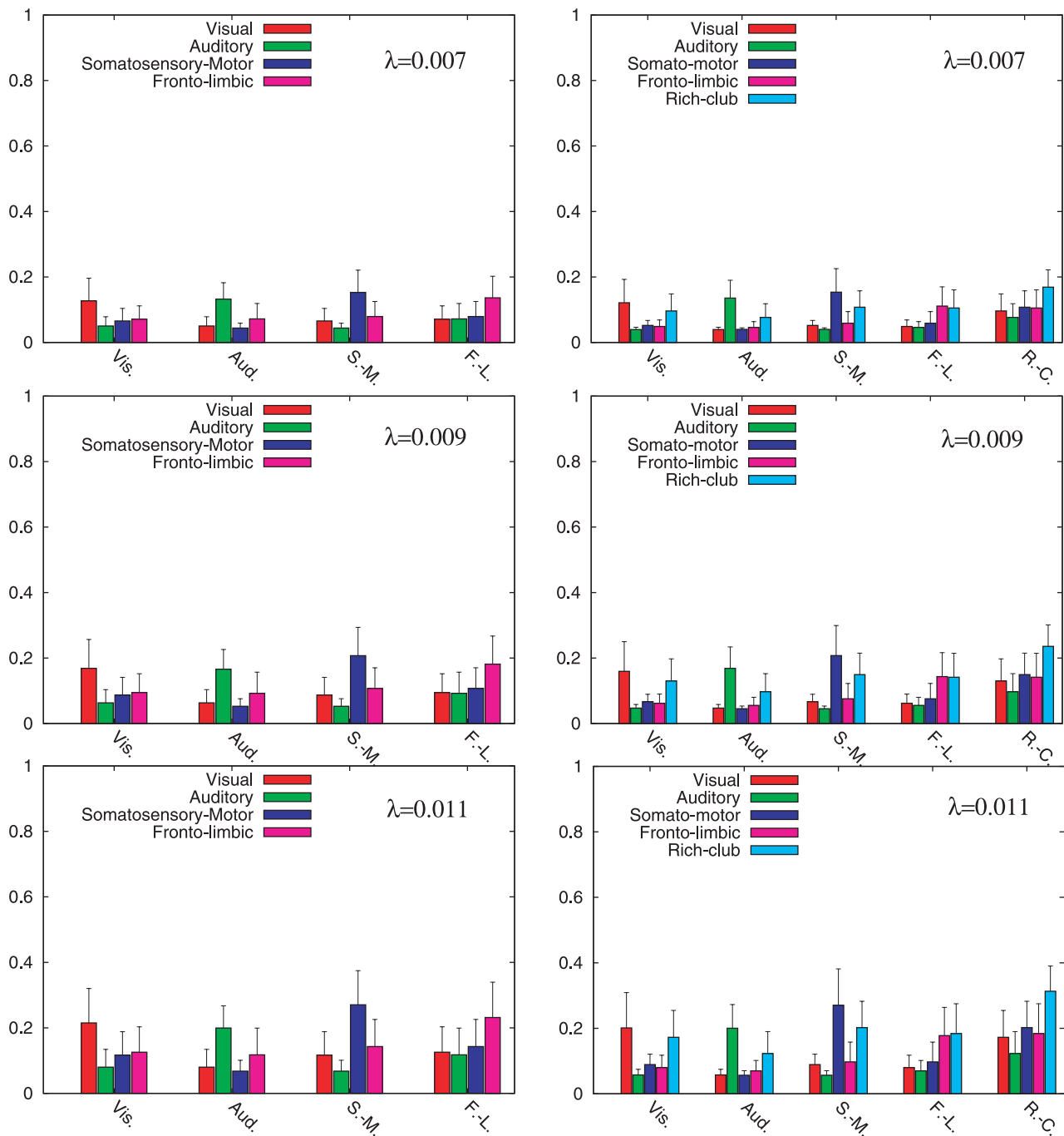


Figure 3. Dynamical correlation within the 4 modal clusters (left column) and the new 4 modally-related clusters and the Rich-Club (right column) before the onset of synchronization. The bars of the histograms show the values of the dynamical correlation $r_{\alpha\beta}$ (see Equation (2)) between the 4 original modules (left) and the new 4 clusters and the Rich-Club (right). From top to bottom we show the cases for $\lambda = 0.007, 0.009$ and 0.011 that correspond to the region before the onset of synchronization. doi:10.1371/journal.pone.0012313.g003

the rest of the network. For instance, at $\lambda = 0.017$ we observe 14 areas spanning from the 36 area to the 2 (Somatosensory-Motor system) while for $\lambda = 0.021$ we find 16 areas ranging from the 36 to the area 4 (Somatosensory-Motor system). From these figures it is no clear that there is one module dominating the synchronization. Quite on the contrary both Somatosensory-Motor and Fronto-Limbic systems are well represented among the most synchronized areas.

A further analysis of the composition of these highly synchronized areas reveals that most of them take part in a higher-order topological structure of the cortical network: a Rich-Club (see Materials and Methods). The Rich-Club of a given network is made up of a set of nodes with high connectivity, which at the same time, form a tightly interconnected community [30,31]. Therefore, the Rich-Club of a network can be described as a highly cohesive set of hubs, that form a dominant community in the hierarchical organization. The

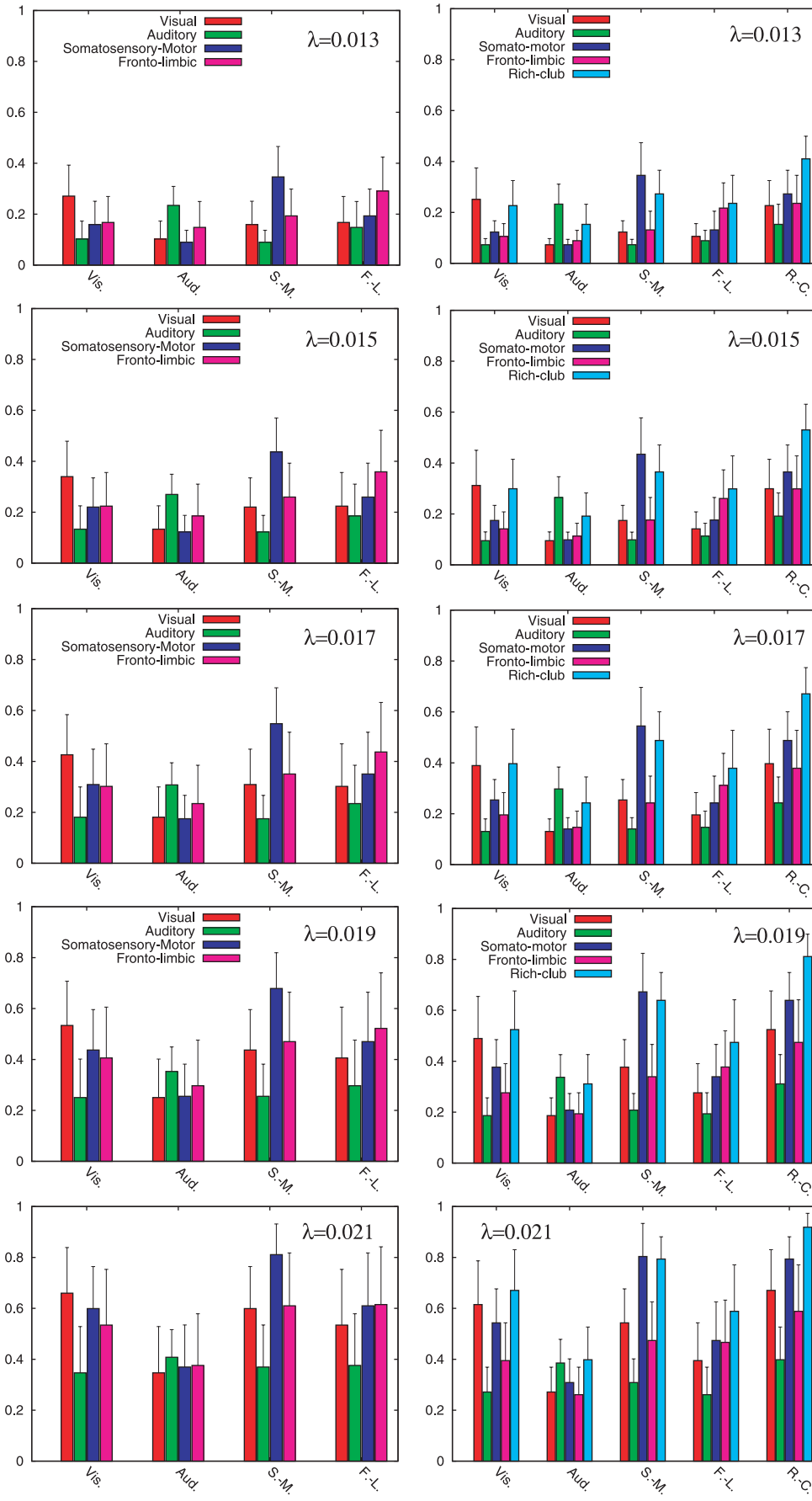


Figure 4. Dynamical correlation within the 4 modal clusters (left column) and the 5 dynamical clusters (right column) at the onset of synchronization. The bars of the histograms show the values of the dynamical correlation $r_{\alpha\beta}$ (see Equation (2)) between the 4 modules (left) and the new 4 modally-related clusters and the Rich-Club (right). From top to bottom we show the cases for $\lambda = 0.013, 0.015, 0.017, 0.019$ and 0.021 that correspond to the onset of synchronization.
doi:10.1371/journal.pone.0012313.g004

Rich-Club of the cat cortex is composed of 11 cortical areas of different modalities: 3 visual areas (*20a*, *7* and *AES*), 1 area from the Auditory system (*EPp*), 2 areas of the Somatosensory-Motor system (*6m* and *5A1*) and 5 fronto-limbic areas (*Ia*, *Ig*, *CGp*, *35* and *36*). In Figure 6 we show again the ranking of areas for the cases $\lambda = 0.015, 0.017, 0.019$ and 0.021 but highlighting those areas belonging to the Rich-Club in black. From the plots it is clear that most of the Rich-Club areas are largely synchronized. In particular for $\lambda = 0.019$ and 0.021 the 8 out of the 10 largest synchronized areas of the network belong to the Rich-Club, although originally they belong to the Fronto-Limbic, Somatosensory-Motor and the Visual systems in the partition into four modules.

Mesoscopic analysis of synchronization including the Rich-Club

Looking at the composition of the Rich-Club we observe that it is mainly composed of fronto-limbic areas. Taking into account

that we previously observed how the Somatosensory-Motor system took the leading role within the description with 4 modules of the synchronization transition, this dominance of the Fronto-Limbic system in the Rich-Club may seem counterintuitive. To test the role of the Rich-Club in the synchronization transition we define a new partition of the cortical network into 5 clusters composed of the Rich-Club (as defined above) and the 4 original modules, but with the corresponding areas of the Rich-Club removed from them.

At the mesoscopic scale, we investigate the self-correlation of the new five clusters and their cross correlation according to Equation (2). In the right columns of Figure 3 and Figure 4 we present the histograms of the inter and intra correlations for different values of the coupling. In both figures the role of the Rich-Club orchestrating the process towards synchrony while increasing the coupling strength becomes clear. More importantly, the addition of the Rich-Club to the partition helps to elucidate the patterns of

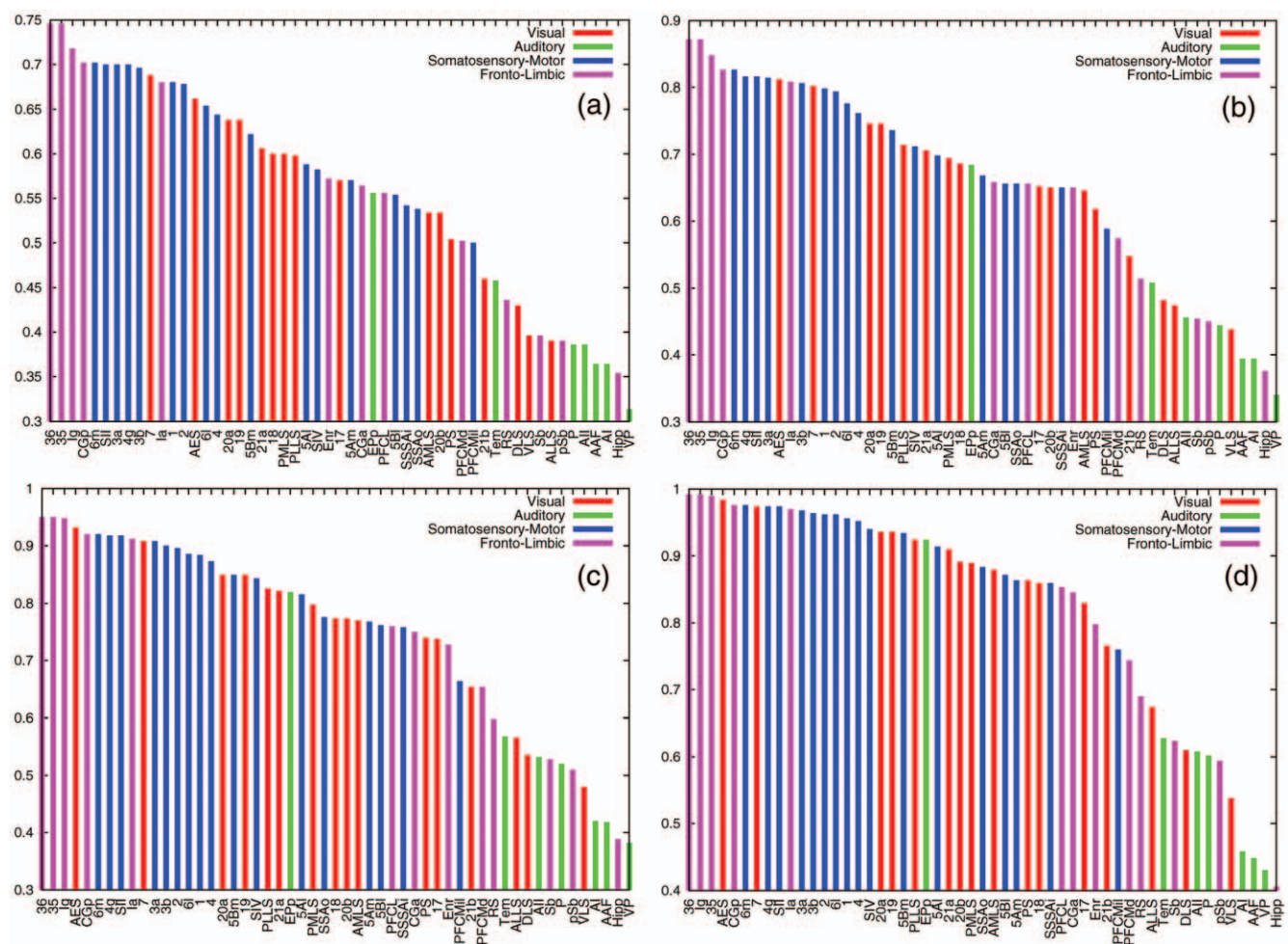


Figure 5. Synchrony Rank of areas: Unveiling anatomical structure of the largest synchronized areas. In these plots we show the rank of areas from the most to the less synchronized for $\lambda = 0.015$ (a), 0.017 (b), 0.019 (c) and 0.021 (d). The height of the bars account of the maximum value of the threshold, T_{ii} , at which the area is incorporated in the synchronized subgraph. Besides, the colour of each bar accounts for the corresponding module of the cortical area.
doi:10.1371/journal.pone.0012313.g005

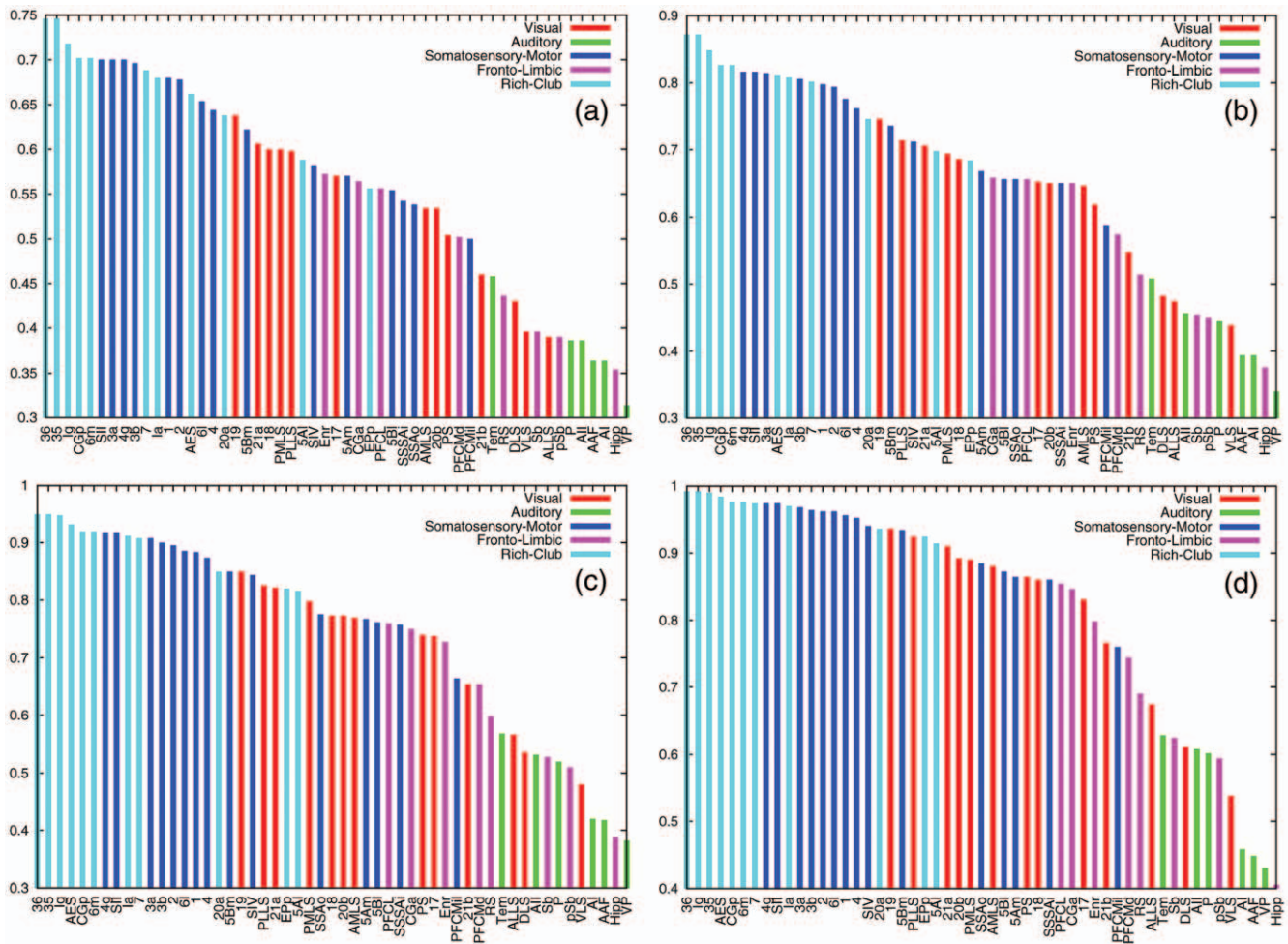


Figure 6. Synchrony Rank of areas: Structure of the largest synchronized areas as described by the Rich-Club. The two plots show the same synchrony ranks as in Figure 5 (again $\lambda = 0.015$ (a), 0.017 (b), 0.019 (c) and 0.021 (d)). We have recolored the bars of those areas corresponding to the Rich-Club to highlight the dominant role of this topological structure in the composition of the largest synchronized areas. doi:10.1371/journal.pone.0012313.g006

synchrony: both the dynamical self-correlation of the four modally-related clusters and their correlation with the Rich-Club remain large. In particular, we observe in Figure 3 that, before the onset of synchronization, these new five modules keep a large self-correlation during this stage. On the other hand, at the onset of synchronization (Figure 4) the four modally-related clusters lose their large self-correlation in the following sequence: The “Fronto-Limbic” cluster remains autocorrelated until $\lambda = 0.013$, the “Visual” one until $\lambda = 0.017$, the “Auditory” system until 0.019 and the “Somatosensory-Motor” cluster until $\lambda = 0.021$. For larger couplings, all the clusters switch from autocorrelation to be synchronized with the Rich-Club, which acts as a physical mean-field of the system. Moreover, during the whole synchronization path the Rich-Club is always the cluster with the largest self-correlation. Thus, the distinction of Rich-Club in the partition preserves the autocorrelation of the four modal clusters before the onset of synchronization while, at the same time, rules the path to complete dynamical coherence during the onset of synchronization. This two-stage dynamics (modal cluster synchronization followed by a sequential synchronization with the Rich-Club) supports the idea that the modular organization with a centralized hierarchy described in [16] facilitates the segregation and integration of information in the cortex.

Characterization of the transition from modular to centralized synchronization

The results so far indicate a plausible transition from modular to centralized organization in the cortex, depending on the coupling strength. In particular, we have shown patterns of synchronization that change the behavior while increasing the coupling λ . Now we propose a characterization of this change in terms of statistical descriptors. To this end, we define two different measures: (i) the dynamical modularity (DM) and (ii) the dynamical centralization (DC). The dynamical modularity compares the degree of internal synchrony within the clusters with the average dynamical correlation across clusters. With this aim we define the DM as the fraction of the average self-correlation of clusters and the average intercluster cross-correlation. For a network composed of m clusters we have:

$$DM = \frac{\sum_{\alpha} r_{\alpha\alpha} / m}{\sum_{\alpha, \beta \neq \alpha} r_{\alpha\beta} / [m(m-1)]}. \tag{3}$$

The DM will take values above 1 when the system contains true dynamical clusters while $DM < 1$ means that the entity of the partition is not consistent with a clustered behavior. On the other

hand, the dynamical centralization of the network measures the relative difference in synchrony between the maximum among the m clusters of $r_x = \sum_{\beta} r_{x\beta}/m$ and the average degree of synchrony over clusters, $\langle r_x \rangle = \sum_x r_x/m$:

$$DC = \frac{\max_x \{r_x\} - \langle r_x \rangle}{\langle r_x \rangle}. \quad (4)$$

In the case of the DC we always obtain positive values. A large value of DC means that the system displays a highly centralized dynamical behavior around a leading cluster while we will obtain DC values approaching 0 when the system behaves homogeneously, *i.e.* when there is no leading cluster that centralizes the dynamics.

We have measured both DM and DC for the original partition into $m=4$ modules and the new partition with $m=5$ incorporating the Rich-Club. In Figure 7 we show the evolution of the two quantities as a function of the coupling parameter. For the case of the DM we confirm that the partition with the Rich-Club keeps the modular behavior of the original partition along the whole synchronization path. The DM is remarkably high for low values of the coupling λ pointing out that before the synchronization onset the internal synchronization dominates over the cross-correlation between the clusters. Regarding the DC we find that in both partitions DC increases with λ reaching a maximum around the synchronization onset, signaling that at this point the synchronization is driven hierarchically and led by one of the modules. However, the partition that incorporates the Rich-Club shows the remarkably larger values of DC along the whole path, specially around the synchronization onset. In particular, the dominant role of the Rich-Club is clearly highlighted by the maximum of the DC at $\lambda=0.015$, just at the onset of synchronization. In order to verify that the Rich-Club is the cluster contributing to the term $\max_x \{r_x\}$ in the dynamical centrality of the network we plot in Figure 7 the evolution of the DC considering each of the 5 modules as the central cluster by substituting $\max_x \{r_x\}$ by the corresponding value of r_x . From the plot it is clear that the Rich-Club is the central cluster orchestrating the dynamics of the system at the onset of synchronization.

The coupled evolution of DM and DC corroborates the two-mode operation of the cortical network when described with the Rich-Club and the remaining parts of the four original modules: At low values of the coupling, the modular structure of the network dominates the synchronization dynamics, pointing out the capacity to concentrate sensory stimuli within its corresponding module. When the coupling is increased the dynamical organization is driven by a leading subset of nodes, organized in a topological Rich-Club, that integrates information between different regions of the cortex.

Discussion

Previous simulations performed in the cat cortical network [23–25] have dealt with its synchronization properties. In these works, the transition towards synchronization is studied by using ensembles of neurons coupled through a small-world topology placed inside each cortical area whereas different neuronal populations are dynamically coupled accordingly to the topology of the cat cortical network. By means of this two-level dynamical model, numerical simulations allowed to find different clusters of synchrony as the coupling between the cortical areas is increased. It was found that only for weak coupling these clusters were closely related to the four modal clusters. In the light of these previous studies, and the recent report of a novel

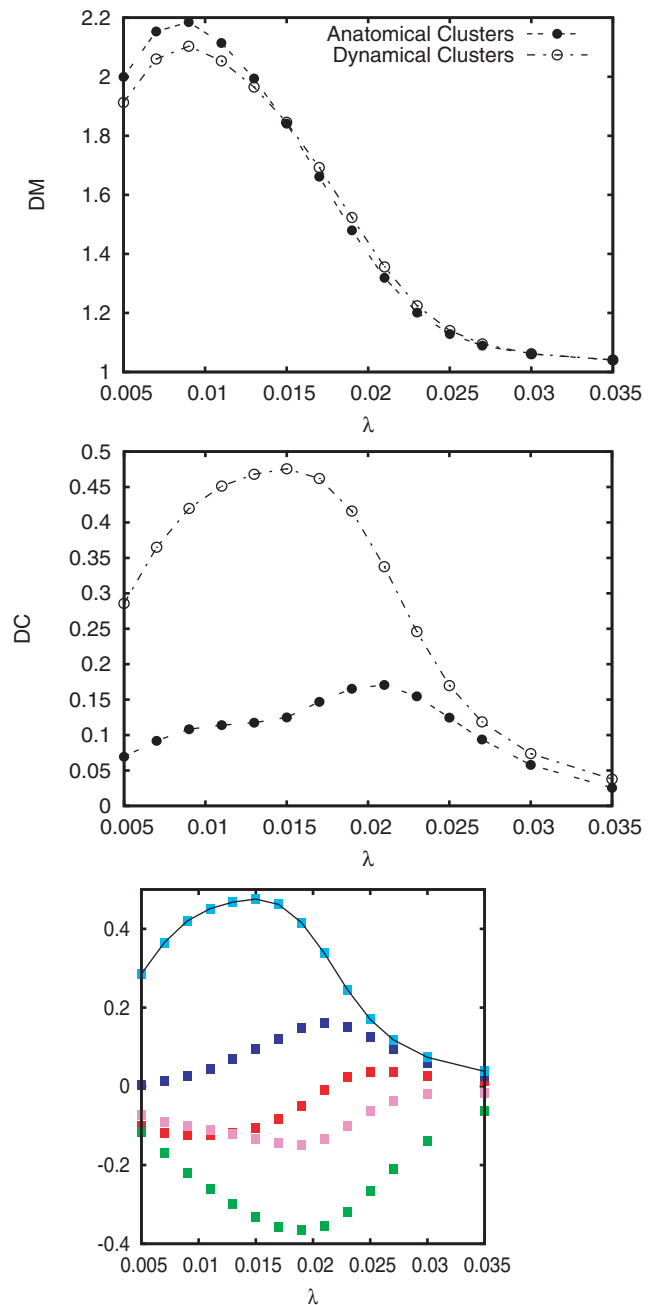


Figure 7. Transition from Modular to Centralized organization of synchronization. The two upper plots show the evolution of the dynamical modularity DM and the dynamical centralization DC as a function of λ . Both panels show the evolution of the above properties for the network described by means of both the original 4 modal clusters and the 5 new modules including the Rich-Club. The panel in the bottom shows the evolution of the DC of the 5 new modules obtained by replacing in Equation (4) the term $\max_x \{r_x\}$ by each r_x corresponding to the new 5 modules. From the curves it is clear that the dynamics is centralized around the Rich-Club. doi:10.1371/journal.pone.0012313.g007

modular and hierarchical organization of the corticocortical connectivity [16], the issue regarding the relation between the mesoscopic structure of the cat cortex and its dynamical organization remains open.

Here, we have investigated the evolution of synchronization in a network representing the actual connectivity among cortical areas

in the cat's brain. We have confirmed, that the role of the different areas in the path towards synchrony is difficult to assess using the traditional partition into four groups of modally-related areas. On the contrary, we have shown that a subset of areas, forming a topological Rich-Club, orchestrates this process. The distinction of this subset permits the interpretation of a new mesoscale formed by the four modules, excluding some nodes that form the Rich-Club, which are considered here as the fifth module. This proposed structure allows us to reveal a transition in the path to synchronization as a function of the coupling strength, that seems to indicate a two-mode operation strategy. For low values of the coupling, a state of weak internal coherence within the five modules governs the coordination dynamics of the network. As the coupling strength is increased, the Rich-Club becomes the responsible of centralizing the network dynamics and leads the transition towards global synchronization.

Finally, the composition of the Rich-Club allows to make some additional biologically relevant observations. First, the Rich-Club comprises of cortical areas of the four different modalities, supporting the hypothesis of distributed coordination dynamics at the highest levels of cortical processing such as integration of multisensory information [32]. Second, the Rich-Club comprises of most of the frontal areas in the Fronto-Limbic module. Moreover, the areas of the Rich-Club collected from the original Somatosensory-Motor system contain the so-called supplementary motor area (SMA). The SMA is a controversial region of the motor cortex, since in contrast with the rest of somatosensory-motor areas it is in charge of the initiation of planned or programmed movements [33]. Furthermore, the area *AES* of the Rich-Club, originally assigned to the Visual module, is believed to integrate all visual and even auditory signals for their multimodal processing and transference as coherent communication signals [34]. Summing up, the Rich-Club is basically made up of areas involved in higher cognitive tasks devoted to planning and integration. The prominent role of the aforementioned regions in the cortex activity is unveiled from our network perspective in terms of a Rich-Club leading the path to synchronization. Our proposal, after this observation, is to investigate the evolution of synchronization in the cat cortex by tracking the transient of five modules corresponding to the anatomico-functional areas (S-M, F-L, Aud, Vis) and the Rich-Club as a separate (but interrelated) functional entities.

Materials and Methods

Cortico-cortical network of cats' brain

After an extensive collation of literature reporting anatomical tract-tracing experiments, Scannell and Young [8,9] published a dataset containing the corticocortical and cortico-thalamic projections between regions of one brain hemisphere in cats. The connections were weighted according to the axonal density of the projections. Connections originally reported as *weak* or *sparse* were classified with 1 and, the connections originally reported as *strong* or *dense* with 3. The connections reported as *intermediate* strength, as well as those connections for which no strength information was available, were classified with 2, see Figure 1(b). Here we make use of a version of the network [10] consisting of $N = 53$ cortical areas interconnected by $L = 826$ directed corticocortical projections.

Rich-Club areas

A key factor of the hierarchical organization of the corticocortical network of the cat is that the hub areas (those with the largest number of projections) are very densely connected between them

[16]. The Rich-Club phenomenon [30,31] is characterised by the growth of the internal density of links between all nodes with degree larger than a given k' , referred as k -density, $\phi(k')$:

$$\phi(k') = \frac{L_{k'}}{N_{k'}(N_{k'} - 1)}, \quad (5)$$

where $N_{k'}$ is the number of nodes with $k(v) \geq k'$ and $L_{k'}$ is the number of links between them. As $\phi(k)$ is an increasing function of k , a conclusive interpretation requires the comparison with random surrogate networks with the same degree distribution. The question is then whether $\phi(k)$ of the real network grows faster or slower with k than the expected k -density of the surrogate networks. If $\phi(k)$ grows slower, it means that the hubs are more independent of each other than expected.

In our case, the network is directed but the input degree $k_{in}(v)$ and the output degree $k_{out}(v)$ of the areas are highly correlated. Hence, we compute the k -density of the corticocortical network of the cat, $\phi_{cat}(k)$, considering the degree of every area as: $k(v) = \frac{1}{2}(k_{in}(v) + k_{out}(v))$. The result is presented in Figure 8 together with the ensemble average $\phi_{1n}(k)$ of 100 surrogate networks. At low degrees $\phi_{cat}(k)$ follows very close the expectation, but for degrees $k > 13$, $\phi_{cat}(k)$ starts to grow faster. The largest difference occurs at $k = 22$, comprising of a set of eleven cortical hubs of the four modalities: visual areas *20a*, *7* and *AES*; auditory area *EPp*, somatosensory-motor areas *6m* and *5A*; and fronto-limbic areas *Ia*, *Ig*, *CGp*, *CGa*, *35* and *36*.

Numerical simulation details

We integrate the Kuramoto equations, see equation (1), using a fourth order Runge-Kutta method with time step $\delta t = 10^{-2}$. The system is set up by randomly assigning the initial conditions $\{\theta_i(0)\}$ and the internal frequencies $\{\omega_i\}$ randomly in the intervals $[-\pi, \pi]$ and $[-1/2, 1/2]$ respectively. The integration of the Kuramoto is performed for a total time $T = 700$. After a transient time of $\tau = 300$ we start the computation of the different dynamical measures such as the order parameters r and r_{link} .

Synchronization order parameters

The dynamical coherence of the population of N oscillators (areas) is measured by means of two different order parameters r and r_{link} . The first one is obtained from a complex number $z(t)$

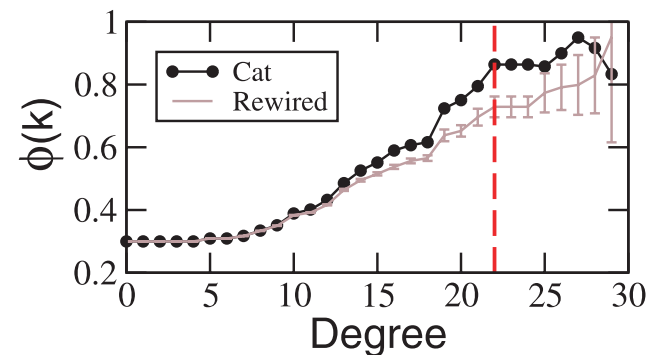


Figure 8. K-density of the corticocortical directed network of the cat $\phi(k)$, compared to the expectation out of the surrogate ensemble. The largest difference occurs at $k = 22$ (vertically dashed line) giving rise to a Rich-Club composed of eleven cortical areas. doi:10.1371/journal.pone.0012313.g008

defined as follows:

$$z(t) = r(t) \exp[i\phi(t)] = \sum_{j=1}^N \exp[i\theta_j(t)]. \quad (6)$$

The modulus of $z(t)$, $r(t)$, measures the phase coherence of the population while $\phi(t)$ is the average phase of the population of oscillators. Averaging over time the value of $r(t)$ we obtain the order parameter $r = \langle r(t) \rangle$.

The second order parameter, r_{link} , is measured looking at the local synchronization patterns, allowing for the exploration of how global synchronization is attained. We define r_{link} by measuring the degree of synchrony between two connected areas i and j :

$$C_{ij} = \lim_{\Delta t \rightarrow \infty} \left| \frac{A_{ij}}{\Delta t} \int_{\tau}^{\tau + \Delta t} e^{i[\theta_i(t) - \theta_j(t)]} \right|, \quad (7)$$

where A_{ij} is the adjacency matrix of the network, being $A_{ij} = 1$ when $W_{ij} > 0$ and $A_{ij} = 0$ otherwise. Each of the values $\{C_{ij}\}$ are bounded in the interval $[0, 1]$, being $C_{ij} = 1$ when the connected areas i and j are fully synchronized and $r_{ij} = 0$ when these areas are dynamically uncorrelated. Note that for a correct computation of C_{ij} the averaging time Δt should be taken large enough (in our computations $\Delta t = 400$) in order to obtain good measures of the degree of coherence between each pair of areas. Since $C_{ij} = 0$ for the areas that are not physically connected we construct the $N \times N$ matrix C and define the global order parameter r_{link} as follows:

$$r_{link} = \frac{1}{L} \sum_{ij} C_{ij}. \quad (8)$$

Therefore, the parameter r_{link} measures the fraction of all possible links that are synchronized in the network.

In the more general case in which all possible pairs of areas are taken into account to compute the average synchronization between cortical areas, Eq.(7) and Eq.(8) can be rewritten as:

$$C_{ij}^* = \lim_{\Delta t \rightarrow \infty} \left| \frac{1}{\Delta t} \int_{\tau}^{\tau + \Delta t} e^{i[\theta_i(t) - \theta_j(t)]} \right|, \quad (9)$$

References

- Engel AK, Singer W (2001) Temporal binding and the neural correlates of sensory awareness. *Trends Cogn Sci* 5: 16–25.
- Engel AK, Fries P, Singer W (2001) Rapid feature selective neuronal synchronization through correlated latency shifting. *Nat Rev Neurosc* 2: 704–716.
- Fahle M (1993) Figure–Ground Discrimination from Temporal Information. *Proc R Soc Lond B* 254: 199–203.
- Singer W, Gray CM (1995) Visual feature integration and the temporal correlation hypothesis. *Ann Rev Neurosci* 18: 555–586.
- Ulhaas PJ, Pipa G, Lima B, Melloni L, Neuenschwander S, et al. (2009) Neural synchrony in cortical networks: history, concept and current status. *Frontiers Int Neurosc* 3: 17.
- Melloni L, Molina C, Pena M, Torres D, Singer W, et al. (2007) Synchronization of neural activity across cortical areas correlates with conscious perception. *J Neurosci* 27: 2858–2865.
- Boccaletti S, Latora V, Moreno Y, eds. (2009) *Handbook on Biological Networks*. Singapore: World Scientific.
- Scannell JW, Blakemore CW, Young MP (1995) Analysis of connectivity in the cat cerebral cortex. *J Neurosci* 15: 1463–1483.
- Scannell JW, Burns GAPC, Hilgetag CC, O'Neill MA, Young MP (1999) The connectional organization of the cortico-thalamic system of the cat. *Cer Cortex* 9: 277–299.
- Hilgetag CC, Burns GAPC, O'Neill MA, Scannell JW, Young MP (2000) Anatomical connectivity defines the organization of clusters of cortical areas in the macaque monkey and the cat. *Phil Trans R Soc London B* 355: 91–110.
- Hilgetag CC, O'Neill MA, Young MP (2000) Hierarchical organization of macaque and cat cortical sensory systems explored with a novel network processor. *Phil Trans R Soc London B* 355: 71–89.
- Sporns O, Chialvo DR, Kaiser M, Hilgetag CC (2004) Organization, development and function of complex brain networks. *Trends Cogn Sci* 8: 418–425.
- Hilgetag CC, Kaiser M (2004) Clustered organization of cortical connectivity. *Neuroinformatics* 2: 353–360.

and

$$r_{link}^* = \frac{2}{N(N-1)} \sum_{ij} C_{ij}^*, \quad (10)$$

respectively. Note that C_{ij}^* and r_{link}^* account for the degree of synchronization between areas i and j regardless of whether or not they are connected.

Defining the average synchronization between areas

To label two areas i and j as synchronized or not one has to analyze the matrix C^* and construct a filtered matrix F whose elements are either $F_{ij} = 1$ if i and j are considered as synchronized or $F_{ij} = 0$ otherwise. From the computation of r_{link}^* , equation (10), one knows the fraction of all possible pairs of areas that are synchronized. Therefore, one would expect that $N(N-1) \cdot r_{link}^*/2$ elements of the matrix F have $F_{ij} = 1$, while the remaining elements are $F_{ij} = 0$. The former elements correspond to the $N(N-1) \cdot r_{link}^*/2$ pairs with the largest values of C_{ij}^* .

In order to measure the average degree of synchronization between pairs of areas one has to average over different n realizations using different initial conditions $\{\theta_i(0)\}$ and different internal frequencies $\{\omega_i\}$ (typically we have used $n = 5 \cdot 10^3$ different realizations for each value of λ studied). To this purpose we average the set of filtered matrices $\{F^l\}$ ($l = 1, \dots, n$) of the different realizations to obtain the average degree of synchronization between areas:

$$r_{ij} = \frac{1}{n} \sum_{l=1}^n F_{ij}^l. \quad (11)$$

In this way the value for $r_{ij} \in [0, 1]$ accounts for the probability that areas i and j are considered as synchronized.

Acknowledgments

The authors are grateful to Jesús Gómez-Tolón for useful discussions and suggestions that helped to improve the manuscript.

Author Contributions

Conceived and designed the experiments: JGG GZL YM AA. Performed the experiments: JGG GZL YM AA. Analyzed the data: JGG GZL YM AA. Contributed reagents/materials/analysis tools: JGG GZL YM AA. Wrote the paper: JGG GZL YM AA.

14. Zamora-López G, Zhou CS, Kurths J (2009) Graphs analysis of cortical networks reveals complex anatomical communication substrate. *Chaos* 19: 015117.
15. Sporns O, Honey CJ, Kötter R (2007) Identification and classification of hubs in brain networks. *PLoS ONE* 10: e1049.
16. Zamora-López G, Zhou CS, Kurths J (2010) Cortical hubs form a module for multisensory integration on top of the hierarchy of cortical networks. *Frontiers Neuroinf*, in press.
17. Hagmann P, Cammoun L, Gigandet X, Meuli R, Honey CJ, et al. (2008) Mapping the Structural Core of Human Cerebral Cortex. *PLoS Biol* 6(7): e159.
18. Arenas A, Díaz-Guilera A, Kurths J, Moreno Y, Zhou CS (2008) Synchronization in complex networks. *Phys Rep* 469: 93–153.
19. Arenas A, Díaz-Guilera A, Pérez-Vicente CJ (2006) Synchronization reveals topological scales in complex networks. *Phys Rev Lett* 96: 114102.
20. Gómez-Gardeñes J, Moreno Y, Arenas A (2007) Paths to synchronization in complex networks. *Phys Rev Lett* 98: 034101.
21. Gómez-Gardeñes J, Moreno Y, Arenas A (2007) Synchronizability determined by coupling strengths in complex networks. *Phys Rev E* 75: 066106.
22. Rulkov NF (2001) Regularization of synchronized chaotic burst. *Phys Rev Lett* 86: 183.
23. Zemanova L, Zhou CS, Kurths J (2006) Structural and functional clusters of complex brain networks. *Physica D* 224: 202–212.
24. Zhou CS, Zemanova L, Zamora G, Hilgetag CC, Kurths J (2006) Hierarchical organization unveiled by functional connectivity in complex brain networks. *Phys Rev Lett* 97: 238103.
25. Zhou CS, Zemanova L, Zamora G, Hilgetag CC, Kurths J (2007) Structure-function relationship in complex brain networks expressed by hierarchical synchronization. *New J Phys* 9: 178.
26. Morgan RJ, Soltész I (2008) Nonrandom connectivity of the epileptic dentate gyrus predicts a major role for neuronal hubs in seizures. *Proc Natl Acad Sci (USA)* 105: 6179–6184.
27. Kuramoto Y (1984) Cooperative Dynamics of Oscillator Community. *Prog Theor Phys* 79: 223–240.
28. Strogatz SH (2000) From Kuramoto to Crawford: exploring the onset of synchronization in populations of coupled oscillators. *Physica D* 143: 1–20.
29. Acebron JA, Bonilla LL, Perez Vicente CJ, Ritort F, Spigler R (2005) The Kuramoto model: A simple paradigm for synchronization phenomena. *Rev Mod Phys* 77: 137–185.
30. Zhou S, Modragón RJ (2004) The rich-club phenomenon in the internet topology. *IEEE Comm Lett* 8(3): 80–182.
31. Colizza V, Flammini A, Serrano MA, Vespignani A (2006) Detecting Rich-Club ordering in complex networks. *Nature Phys* 2: 110–115.
32. Bressler SL, Kelso JAS (2001) Cortical coordination dynamics and cognition. *Trends Cogn Sci* 5: 26–36.
33. Nachev P, Kennard Ch, Husain M (2008) Functional role of the supplementary and pre-supplementary motor areas. *Nature Rev Neuroscience* 9: 856–869.
34. Stein BE, Stanford TR (2008) Multisensory integration: current issues from the perspective of the single neuron. *Nature Rev Neuroscience* 9: 255–266.